JPE 19-6-9

https://doi.org/10.6113/JPE.2019.19.6.1440
ISSN(Print): 1598-2092 / ISSN(Online): 2093-4718

Graphical Design Plane Analysis for Series-Compensated Resonant Energy Links of Inductive Wireless Power Transfer Systems

Chae-Ho Jeong* and Sung-Jin Choi†

†,*School of Electrical Engineering, University of Ulsan, Ulsan, Korea

Abstract

In wireless power transfer systems, it is important to design resonant energy links in order to increase the power transfer efficiency and to obtain desired system performances. This paper proposes a method for designing and analyzing the resonant energy links in a series-series configured IPT (inductive power transfer) system using the FOM-rd plane. The proposed FOM-rd graphical design plane can analyze and design the voltage gain and the power efficiency of the energy links while considering changes in the misalignment between the coils and the termination load condition. In addition, the region of the bifurcation phenomena, where voltage gain peaks are split over the frequency, can also be distinctly identified on the graphical plane. An example of the design and analysis of a 100 W inductive power transfer system with the proposed method is illustrated. The proposed method is verified by measuring the voltage gain and power efficiency of implemented hardware.

Key words: Design plane analysis, Figure of merit (FOM), Inductive power transfer (IPT), Series-series configuration, Wireless power transfer (WPT)

I. INTRODUCTION

Inductive power transfer (IPT) technology improves both safety and convenience. In addition, it results in a waterproof system since metal contacts can be omitted. Generally, IPT utilizes Faraday induction between two adjacent magnetically coupled coils that are located remotely. In order to increase the power transfer efficiency in practical applications, the coils are compensated by capacitors in series or in parallel, which together constitute a pair of resonant energy link structures [1]-[3]. Such a resonant structure can be categorized into series-series (S-S), series-parallel (S-P), parallel-series (P-S), and parallel-parallel (P-P) configurations, as shown in Fig. 1. In addition, a typical IPT system in the S-S configuration is shown in Fig. 2.

The resonant energy link structure determines the overall performance of an IPT system. Thus, complete understanding of the mechanism is so crucial that many researches have been focused on the characteristics of the energy link structures [4]-[8]. The mathematical analysis based on coupling theory in [9] presents a fundamental theoretical background to the resonant energy link. However, all of the performance factors are represented by scattering parameters that are unfamiliar to power electronics engineers. In a circuit-oriented manner, a number of circuit equations were solved in [10] to describe the energy link.

However, the equation-based approach is too complex and is not very intuitive. Therefore, it is very difficult to determine the influences on performance due to variations of the load resistance or the magnetic coupling coefficient. Either of these can be caused by perturbations in the coil alignment or distance. Some recent researches have attempted to improve the design procedure. For example, the authors of [12] suggested a method to bring application-level criteria into the coil design of an IPT system. However, the contribution of this study was limited to a specific tri-spiral repeater. The authors of [13] proposed another systematic design procedure that utilizes a singular point having a constant voltage gain regardless of the load. However, it still resorts to complex equations and does not take the coupling coefficient variation into account. From a survey of the literature, it can be seen that few studies have

Manuscript received Feb. 7, 2019; accepted Aug. 15, 2019
Recommended for publication by Associate Editor Byoung-Hee Lee.
†Corresponding Author: sjchoi@ulsan.ac.kr
Tel: +82-52-259-2716, Fax: +82-52-259-1687, University of Ulsan
*School of Electrical Engineering, University of Ulsan, Ulsan, Korea

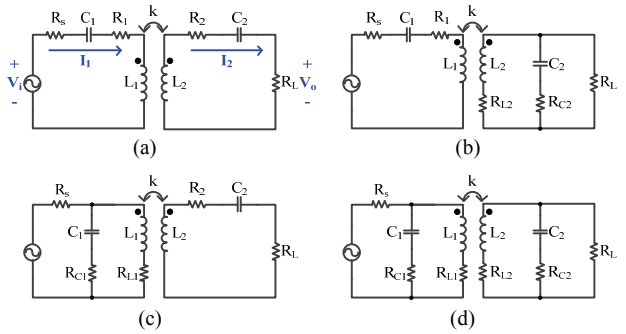

Fig. 1. Resonant structures in IPT. (a) S-S. (b) S-P. (c) P-S. (d) P-P.

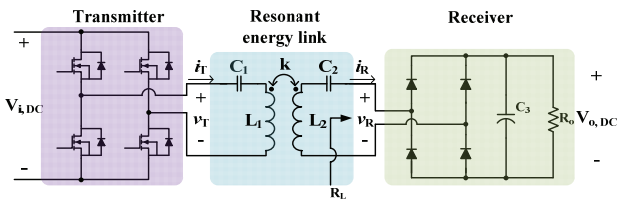

Fig. 2. Typical IPT system in the S-S configuration.

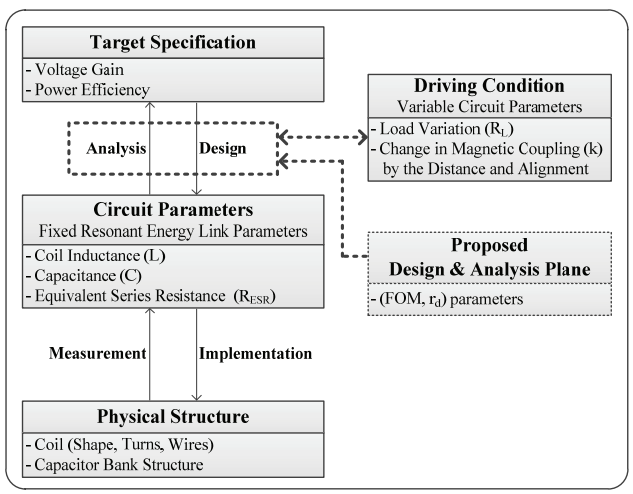

Fig. 3. Design and analysis flow for an IPT resonant energy link.

investigated an effective method for the design and analysis of wireless energy links from the perspective of circuit engineers.

Fig. 3 summarizes the general flow of the design and analysis for the energy link. In terms of design process, starting from the target performances such as the voltage gain or power efficiency, the circuit parameters need to be determined. Subsequently, the physical structures of the coils and resonant capacitors are implemented by an inductance formula or field analysis tools. On the other hand, analysis is the reverse process. By measurements with the wireless energy link structure, the circuit parameters are extracted by fitting the measurement data to a lumped equivalent model. Then the performance can be calculated by circuit simulation. It is obvious that either the analysis or the design requires a number of iterations since it should be performed in the light of both the load variation and the alignment condition that alters

TABLE I
NOMENCLATURES

Symbols	QUANTITIES
L_1, L_2	self-inductances of Tx and Rx resonator
C_1, C_2	compensation capacitors for Tx and Rx resonator magnetic induction
R_1, R_2	total ESR's for Tx and Rx resonator
R_s	internal resistance of the voltage source
R_L	equivalent load resistance
k_1, k_2	coupling coefficients with regard to Tx and Rx
k	geometric mean of k_1 and k_2
ω	operating angular frequency
ω_o	resonant angular frequency of resonator
Z_{o1}, Z_{o2}	characteristic impedances of Tx and Rx, $Z_{o1}=(L_1/C_1)^{1/2}$, $Z_{o2}=(L_2/C_2)^{1/2}$
Q_1, Q_2	quality factors of Tx and Rx resonator, $Q_1=Z_{o1}/R_1$, $Q_2=Z_{o2}/R_2$
Q	geometric mean of Q_1 and Q_2

coupling coefficient. A large number of computer simulations are sometimes useful. However, they are not very insightful from the engineer's point of view. In order to develop alternative ways of design and analysis without a loss of generality, multiple aspects including the characteristics of energy link, the load condition, and use scenarios such as the distance or alignment between the source and the target object, should be considered at the same time. In an effort to resolve these issues, [14] introduced a two-dimensional (2-D) normalized plane called the figure-of-merit-r_d (FOM-r_d) plane, and presented a new graphical design and analysis method on this plane. This method offers circuit engineers both convenience and insight. This paper is an extension of this original work, and includes more analytical considerations and additional verifications through hardware experiments to support the proposed methodology.

This paper is organized as follows. A theoretical formulation with its physical meaning are presented in Section II. Hardware verification results are discussed in Section III to check the validity and effectiveness of the proposed method. Finally, some conclusions are drawn in Section IV.

II. PROPOSED DESIGN PLANE

A. Theoretical Derivation

Fig. 1(a) shows an AC equivalent circuit of an IPT system in the S-S topology, which is popular in most applications. In this figure, V_i, I_1 and I_2 are phasor representations of the input voltage, the transmitter (Tx) current, and the receiver (Rx) current, respectively. The circuit parameters used in the mathematical formulation are summarized in Table I. It should be noted that the equivalent series resistances (ESR) such as R_1 or R_2 are the sum of the individual ESRs in the coil as well as the compensation capacitor. To describe the characteristics of the energy link, the quality factor is defined

as the characteristic impedance divided by the ESR. If the resonant frequencies of Tx and Rx are the same and the drive frequency is equal to the resonant frequency, the linear relation between the phasors can be obtained as follows:

$$\begin{bmatrix} \mathbf{V_i}/(R_s+R_1) \\ 0 \end{bmatrix} = \begin{bmatrix} -j\frac{Q_1}{1+R_s/R_1}(\omega_N^{-1}-\omega_N^2)+1 & j\omega_N k_1 \frac{Q_1}{1+R_s/R_1} \\ j\omega_N k_2 \frac{Q_2}{1+R_L/R_2} & -j\frac{Q_2}{1+R_L/R_2}(\omega_N^{-1}-\omega_N^2)+1 \end{bmatrix} \begin{bmatrix} \mathbf{I_1} \\ \mathbf{I_2} \end{bmatrix} \quad (1)$$

Since it is necessary to simplify the subsequent formulation, three assumptions are made. First, the transmitter and the receiver energy links are symmetric: $L_1 = L_2 = L$, $C_1 = C_2 = C$, $R_1 = R_2 = R$, $k_1 = k_2 = k$ and $Q_1 = Q_2 = Q$. Secondly, the switching devices are nearly ideal. Thus, the source impedance is sufficiently small to be ignored: $R_s = 0$. Lastly, the operating frequency of the system is the same as the resonant angular frequency of the circuit, $\omega_N = 1$.

The main objective of this paper is to make the design and analysis of an IPT resonator simple and intuitive. There are a lot of parameters to characterize the energy link in an IPT system. As a result, it is not easy to consider all the parameters at the same time. Therefore, most of the important performance indices are represented in view of two-dimensional parameter plane. Undoubtedly, the performance index should be the voltage gain and the power efficiency. Meanwhile, it is rather difficult to choose the parameter space. Eventually, it is concluded that the two normalized axis variables, FOM and r_d, are effective for the parameter space, where the former describes the energy link characteristics and the latter represents the load termination conditions. These variables are defined by:

$$FOM \equiv kQ, \quad r_d \equiv \frac{R_L}{R}. \quad (2)$$

The figure of merit, FOM, is obtained by multiplying the coupling coefficient, k, and the quality factor Q of the coil. In addition, r_d is the ratio of the load resistance to the internal loss resistance of the resonator. From the mathematical analysis presented in this paper, it is known that the voltage gain and the power efficiency are completely and uniquely described by the FOM and r_d, not by individual values of k or Q. Thus, it is feasible to combine them into a single parameter, FOM. Therefore, any effect on the performance index caused by a change in the coupling coefficient or a modification of the coil structure can be described solely by the FOM. Likewise, any change in the load condition can be describe by r_d.

Utilizing (2), the key performance indices are derived from (1), where the detailed process is explained in Appendix A. The AC voltage gain of the resonant link is given by formula (3).

$$M_{V,AC} = \frac{FOM \cdot r_d}{FOM^2 + (1+r_d)} = f(r_d, FOM) \quad (3)$$

Similarly, the power transfer efficiency of the resonant energy link is formulated in (4).

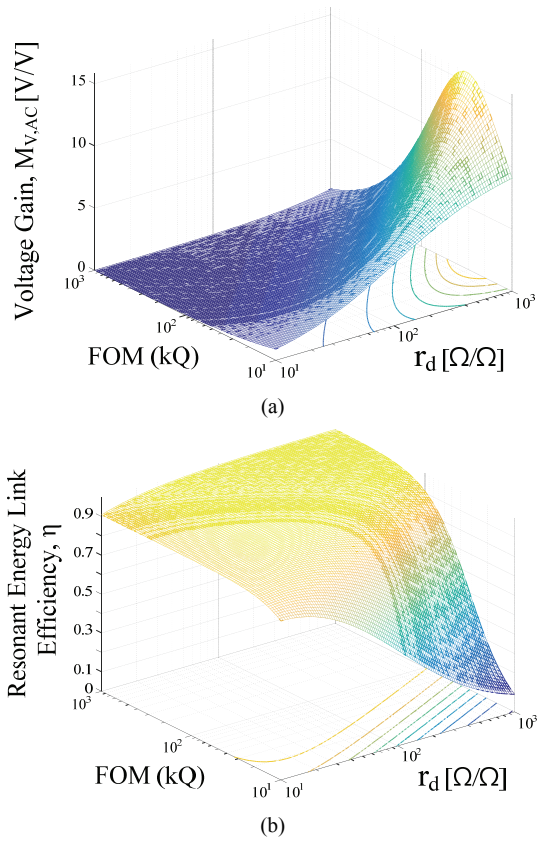

Fig. 4. Performance indices in the FOM-r_d plane. (a) Voltage gain. (b) Efficiency.

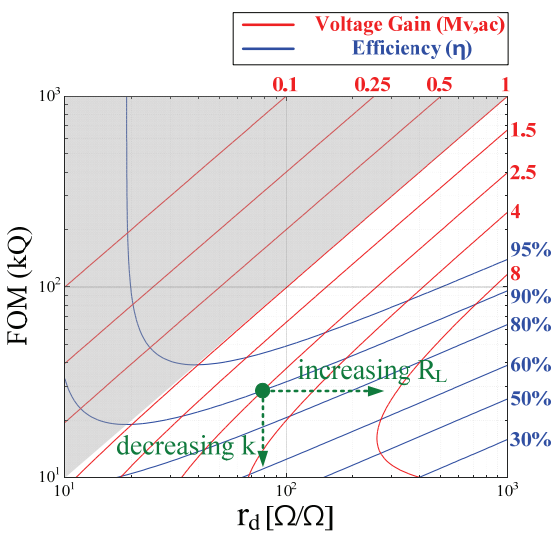

Fig. 5. FOM-r_d design plane.

$$\eta = \frac{FOM^2 \cdot r_d}{(1+r_d)^2 + FOM^2(1+r_d)} = g(r_d, FOM) \quad (4)$$

Since both (3) and (4) are functions of FOM and r_d, it is obvious that the key performance indices can be mapped on the plane of FOM-r_d. Figs. 4(a) and 4(b) show the surface plots in the FOM-r_d plane that describe the voltage gain and the efficiency, respectively. Fig. 5 shows a contour plot

representing two performance indices on the same plane, which plays a critical role in the analysis and design of the resonant energy link.

The proposed method is different from the conventional approach due to two major features. First, it combines two different perspective of tasks: circuit design and coil design. Hence, it is suitable for the system-level design of a WPT system. Secondly, the bifurcation region is graphically shown, which makes it easy to avoid the region. There have been many papers on IPT system from the point of view of the design and analysis procedures. In [9] and [10], equivalent circuits are adopted to calculate the power efficiency to find the maximum efficiency condition of a particular coil shape. In addition, they handled circuit design and coil design separately. For example, circuit-oriented design regards the magnetic energy link as a given structure and derives the maximum efficiency condition by circuit theory. The voltage gain is obtained later and the resonant capacitor is designed based on the operating frequency. Meanwhile, coil-oriented design struggles with the coil structure to maximize the power transfer efficiency based on network theory. However, both lack a systematic consideration from the perspective of design flow. The two approaches should be combined since the coil design needs to be modified to achieve the required voltage gain, or the voltage gain should be adjusted to compensate any limitations due to the coil structure. Similarly, there have been a few papers like [16] that discuss the gain bifurcation criterion. However, it can be difficult to get any design idea directly from the conditions during the design phase with the conventional method.

When the resonant energy link specifications are expressed by FOM and r_d, the voltage gain and power efficiency can be expressed in a two-dimensional graph as shown in Fig. 5 without losing much information. This makes the analysis and design simpler and more intuitive. Fig. 3 shows the flow of the design and analysis, which demonstrates the feasibility of the proposed idea. When the target specifications of the resonant energy link are defined as the voltage gain and power efficiency, they are intuitively able to convert the voltage gain and efficiency into circuit parameters while considering changes of the load (R_L) and coupling coefficient (k) through the proposed plane. The resonant energy link can be implemented later through the determined circuit parameters. On the other hand, the performance of the existing resonant energy link can be analyzed according to load variations or to any change that might affect the magnetic coupling coefficient such as the distance or misalignment between two coils.

The following sections explain the usefulness of the proposed method in terms of the analysis and design process, respectively.

B. Analysis via FOM-r_d Plane

By directly calculating FOM and r_d for a ready-made energy link structure, it is possible to locate the operating point. In addition, the proposed FOM-r_d plane provides an intuitive way to understand the performance dependency on external conditions such as the load resistance, degree of misalignment and coil distance variation effects. For example, if the load resistance R_L increases, the operating point shifts to the right, as shown in Fig. 5, causing an increased voltage gain and a decreased voltage gain. On the other hand, when the distance between the Tx and Rx coils increases, the degraded coupling coefficient forces the operating point to shift further downward, as shown in Fig. 5.

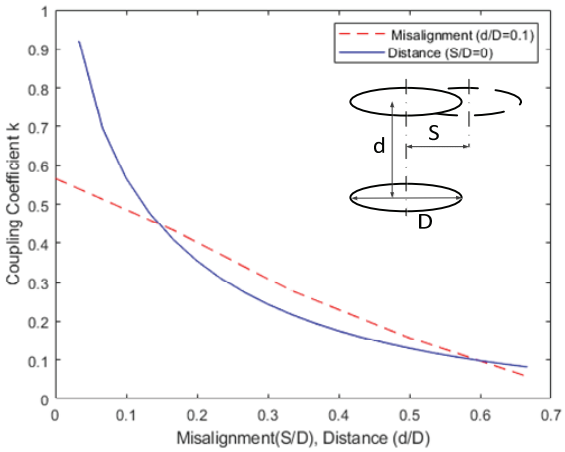

Fig. 6. Coupling coefficient vs. physical arrangement of coils.

Actually, with a given coil, any change in the physical arrangement can be mapped to the FOM axis. Fig. 6 shows the dependency between the physical arrangement and the coupling coefficient in the case of a circular planar coil [11]. This shows that the coupling coefficient, k, decreases as the distance, d, between two coils increases. In similar ways, the greater the lateral misalignment, S, the less the coupling coefficient becomes. Likewise, it is also possible to consider the angular tilt of a coil, as mentioned in [8], if the change in the coupling coefficient is mapped to the proposed FOM-r_d graph to find the voltage gain and efficiency according to the angle. Therefore, any physical disposition that affects the magnetic coupling coefficient such as the distance, misalignment and angular tilt between two coils can be associated with the proposed method.

Another advantage of the FOM-r_d plane analysis is that the peak splitting phenomenon in the voltage gain, which is referred to as bifurcation, can be graphically detected. The gain bifurcation is a challenge in frequency-controlled output regulation mechanisms. Sometimes it hampers the soft-switching operation of Tx inverter power switches. The criterion to prevent the occurrence of bifurcation in the S-S configuration can be simplified to the following inequality:

$$FOM < r_d. \tag{5}$$

The proof of (5) is given in Appendix B. The above condition can be mapped onto the lower right un-shaded

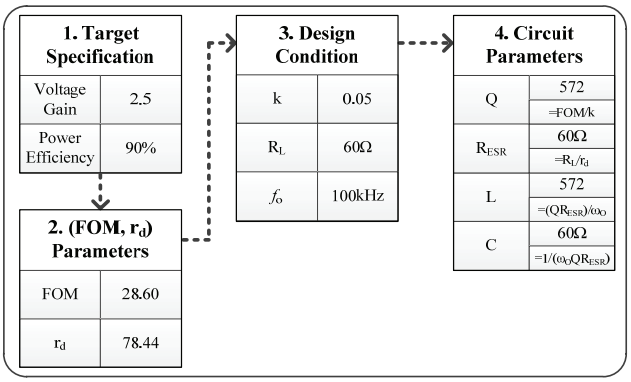

Fig. 7. Process of circuit parameter calculation.

region in the FOM-r_d plane as shown in Fig. 5. Clearly, in order to guarantee such a bifurcation-free operation, it is necessary to confine the operating point to this region over the entire range of load resistance and magnetic coupling conditions.

C. Design via FOM-r_d Plane

The FOM-r_d plane is convenient, especially for the resonant energy link design process. If the voltage gain and load resistance are specified with a power efficiency guideline, the energy link can be designed by selecting (r_d, FOM) in the FOM-r_d plane. In the first phase of the design process, the minimum quality factor of the coil and the maximum internal loss of the resonator are calculated to achieve the initial power efficiency goal. However, it is not always possible to achieve such a high Q or low R due to physical limitations such as the coil thickness or material properties. Therefore, it is necessary to relocate the (r_d, FOM) coordinate along the constant voltage gain trajectory with a lower power efficiency goal (which is the lower left direction in Fig. 5). When a new coordinate is eventually found, this point determines the physically achievable power efficiency, and the coil inductance and the capacitance are calculated by (6).

$$Q=\frac{FOM}{k},\quad R=\frac{R_L}{r_d},\quad L=\frac{QR}{\omega_O},\quad C=\frac{1}{\omega_O QR} \tag{6}$$

Therefore, it is possible to design the circuit parameters of the resonant link by the voltage gain and efficiency specification. The design flow is summarized in Fig. 7 for better understanding. Afterwards, the physical coil arrangements can be implemented based on the circuit parameters utilizing an inductance formula that will be shown in Section III.

By the way, it should be noted that when a system approaches the full load condition, the operating point tends to shift further into the region of bifurcation. Likewise, as the degree of coil misalignment or the distance between coils decreases, the energy link becomes more prone to bifurcation. Therefore, if an IPT system with a varying load resistance or coupling coefficient is to be designed, it is necessary to start the design under a full load and at the maximum coupling coefficient in order to guarantee the uniqueness of the voltage gain peak.

III. Verification of the Proposed Method

A. Design Example and Experiment Results

1) Design Condition and Simulation Results: In this section, the hardware design of a 100W energy link structure for an IPT system shown in Fig. 2 is described in order to verify the FOM-r_d plane. The design follows the process shown in Fig. 7. The target voltage gain is 2.5 and the load resistance, R_L is 60Ω. According to Fig. 5, along the line of $M_{V,AC}$ = 2.5, an energy link with larger values in both FOM and r_d indicates a higher power transfer efficiency. However, the maximum achievable efficiency is usually limited by the ESR of the resonators. Thus, the target efficiency is set to 90%. From the FOM–r_d plane in Fig. 5, the green dot (FOM = 28.60 and r_d = 78.44) is selected to meet the specifications. When the magnetic coupling coefficient, k, is assumed to be 0.05 and the resonant frequency of the system, f_o, is set to 100kHz, the circuit parameters are calculated as Q = 572, R = 765mΩ, L = 696uH, and C = 3.64nF using (6).

Circuit simulation (LTSpice, Linear Technology) is used to verify that the circuit parameters obtained from the green dot meet the target specifications. Based on the above draft design by the FOM-r_d plane, simulation results show that the voltage gain and efficiency are 2.5 and 90%, respectively, which is consistent with the target specifications. Through the simulation of the output power 100W, the Tx-side capacitor and coil show a voltage stress and a current stress of 1.4kV and 3.3A in magnitude, respectively. In addition, the Rx-side capacitor and coil undergo a voltage stress and a current stress of 0.42kV and 0.93A in magnitude, respectively.

2) Coil Design: The coils used for the hardware verification are formed from spiral windings with a square cross-section. Fig. 8 shows a cross-sectional view of the coils being designed. They have a 30cm mean coil diameter and are appended by a 30cm x 30cm x 0.5cm square ferrite plate. Since the voltage stress in the coil is relatively high at 1.4kV, acrylic insulation layers are inserted to avoid electrical breakdown between the windings. To ensure that the coupling coefficient is k = 0.05, the Tx and Rx coils are placed 25cm apart, which is found using finite element analysis (FEA) with FEMM v4.2. Then it is slightly adjusted experimentally.

The inductance formula in [15] is utilized to implement a practical coil structure, where the value of the inductance is 696uH. The inductance calculation is carried out by Stefan's formula (7), (8):

$$S(r,N)=4\pi\left[\frac{1}{2}\left\{1+\frac{1}{6}\left(\frac{b}{2a}\right)^2\right\}ln\frac{8}{\left(\frac{b}{2a}\right)^2}-0.84834+0.2041\left(\frac{b}{2a}\right)^2\right], \tag{7}$$

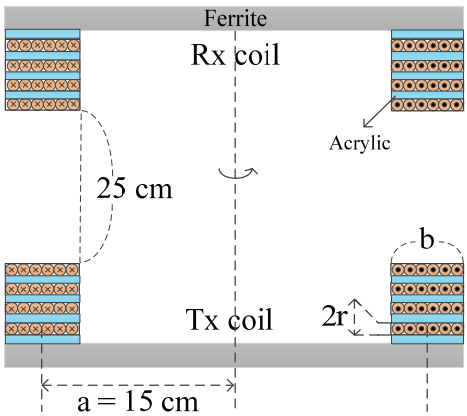

Fig. 8. Physical arrangement of the IPT coils to be designed.

$$L = 0.1aN^2 S(r, N) \quad [\text{uH}]. \tag{8}$$

where the values of a, b, r and N represent the mean radius in cm, the length of the coil cross-section in cm, the conductor size in mm, and the number of turns, respectively.

The target ESR value of the coil is obtained by subtracting the ESR of the capacitor bank from the total ESR value. In this coil implementation, the ESR of the capacitor bank is assumed to be zero. Thus, the target ESR value of the coil is calculated as 765mΩ. Even though the total wire resistance increases significantly more than the DC static resistance with high frequency operation, adopting a Litz-wire to suppress the skin effect leads to a moderate increase in the resistance. Considering the margin and accounting for the proximity effect, the target DC resistance is empirically designed to be about 100mΩ, using the formula given in (9).

$$R_{DC}(r, N) = 2\rho \frac{aN}{r^2} \quad [\Omega] \tag{9}$$

Therefore, the coils are made of Litz-wire with a 1.2mm diameter and 34 turns, (N = 34). Based on the above design, the inductances of the implemented coils are L_1=615.0uH and L_2=614.0uH, when measured by an LCR meter (4263B, Agilent). Therefore, the capacitance value is adjusted to 4.12nF to fix the resonant frequency to 100kHz.

3) Capacitor Design: Since the resonant energy link requires a very high-quality factor, it is necessary to consider the voltage stress of the capacitor (1.4 kV for Tx and 0.42 kV for Rx). As a result, high voltage film capacitors (ICEL, PSB2301680KGS) are used in the 6S-4P configuration.

The capacitor bank structure consists of both a series and a parallel connection. This is due to the fact that the voltage and current stresses of the Tx-side capacitor must be considered. Consequently, high voltage film capacitors (ICEL, PSB2301680KGS) are used in the 6S-4P configuration. According to the capacitor datasheet, this component has a 6.8nF capacitance that endures 750V (RMS), and the ESR of the capacitor at 100kHz is found to be 64mΩ. Thus, the capacitor bank carries a total capacitance of 4.53nF with

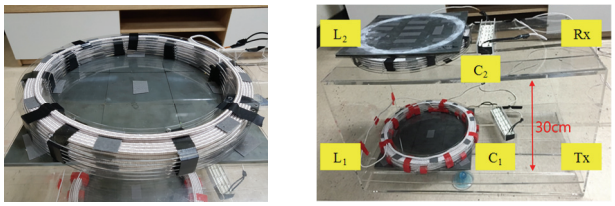

(a) (b)

Fig. 9. Implementation of the: (a) Rx coil, (b) Resonant link.

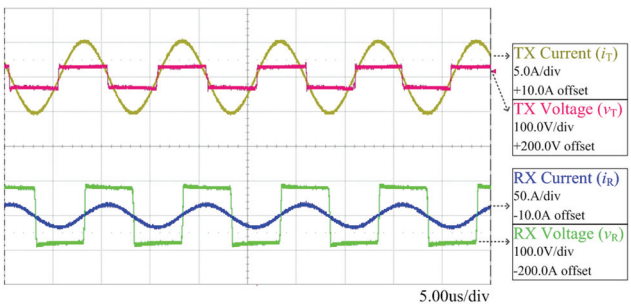

Fig. 10. Operating waveforms of the designed resonant energy link.

96mΩ ESR and it can withstand a maximum of 1.4kV. The same configuration is used for the Rx-side capacitor bank. As a result, the measured capacitance values are C_1 = 4.12nF and C_2 = 4.14nF. To make the resonance frequency close to 100kHz, the coil winding is slightly adjusted to match the resonant frequency between Tx and Rx. Therefore, the average coil inductance is 613uF. The implemented coil and the resonant energy link comprising the designed capacitor banks and coils are shown in Figs. 9(a) and 9(b), respectively.

4) Experiment Results: The overall system, which contains the resonant link, is tested with a full-bridge inverter for the Tx-side, and a full-wave diode rectifier for the Rx-side. The voltage gain and power efficiency of the implemented resonant energy link structure are measured by a power analyzer (PPA 5530, N4L). The DC load resistance is set to 74Ω, which can be reflected into the resonant energy link as an equivalent AC load resistance of 60Ω, considering the effect of the full-wave rectifier. When the DC input voltage is 30.0V, the DC output voltage is 77.7V. By a fundamental harmonic approximation, the contributions of the full-bridge inverter in the TX and the full-wave rectifier in the RX cancel each other out, which makes the AC voltage gain, $M_{V,AC}$ equal to the DC voltage gain. An experiment waveform is shown in Fig. 10. In this figure, v_T and i_T are the primary voltage and current, and v_R and i_R are the secondary voltage and current, where the circuit variables are defined in Fig. 2. The voltage gain is measured as 2.59 and the output power is 100.6W. The power efficiency is measured to be 88.10%. The differences between the designed and measured values are 3.6% in the voltage gain and 1.2% in the power efficiency, which can be acceptable in the draft design phase. The errors are mainly caused by the difficulty of exact ESR implementation. For example, the measured voltage gain and power efficiency are equivalent to

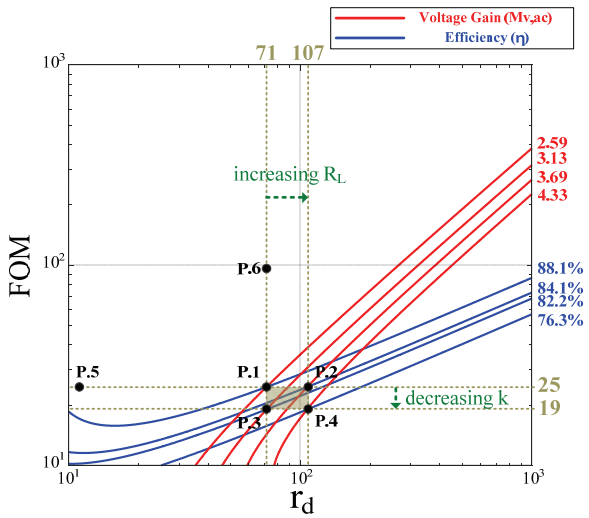

Fig. 11. Operating points (Pont 1 to Point 6) of the resonant energy link mapped on the proposed plane.

the point of (r_d, FOM) = (71.4, 24.6) in the normalized plane, which corresponds to R_{ESR} of 1.19Ω by Eq. (6). This is about 1.6 times higher than the original target value of 765mΩ, which increases both r_d and the quality factor. As a result, the original design point of (r_d, FOM) = (78.44, 28.60) was shifted toward the upper-right direction by 1.6 times. This tendency matches well with the original theoretical analysis results, which validates the design process of the wireless energy link.

B. Analysis Example and Experiment Results

Another experiment is made to demonstrate the analysis process using the FOM-r_d plane, where the voltage gain, efficiency, and bifurcation condition can be analyzed. If the use scenario is set up and the range of both the equivalent load resistance R_L and the magnetic coupling coefficient are given, the region of operation needs to be confined to a rectangle in the FOM-r_d plane. Accordingly, it is possible to analyze the voltage gain, power efficiency and bifurcation occurrence under the operating conditions.

For a hardware test, the pair of the Tx and Rx resonant energy link constructed in the previous section are regarded as a ready-made energy link. At first, their quality factor and ESR are measured, which shows 473 and 1.19Ω, respectively. The rectangular region in Fig. 11 shows the operating area when the load resistance of the system changes from 60Ω to 90Ω (+50% increase) and the coupling coefficient varies from 0.051 (distance 25cm) to 0.041 (distance 30cm). The coordinate (r_d, FOM) values of the four corner points (Points 1-4) are as follows: (71.4, 24.6), (107.1, 24.6), (71.4, 19.0) and (107.1, 19.0). The corresponding voltage gains and power efficiencies are (2.59, 88.1%), (3.69, 84.1%), (3.13, 82.2%) and (4.33, 76.3%), respectively. Therefore, it can be predicted in advance that the voltage gain will vary from 2.59 to 4.33 and that the power efficiency will vary from 76.3% to

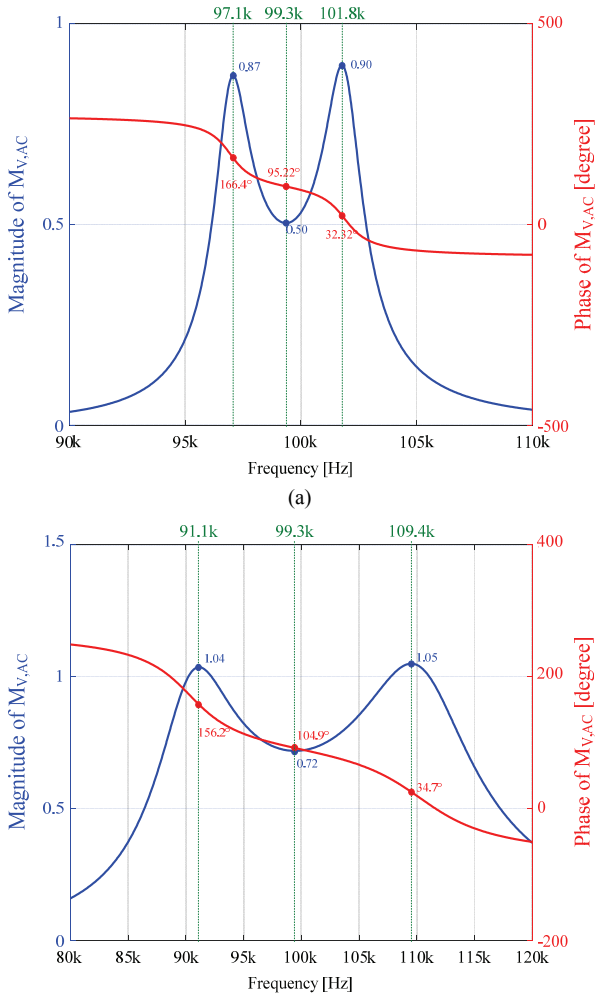

Fig. 12. Voltage gain plots by a frequency analyzer at: (a) Point 5, (b) Point 6.

88.1% under the given operating conditions.

To experimentally verify above prediction, the voltage gains and the power efficiencies are measured through a power analyzer (PPA 5530, N4L) when the IPT system is operated at Point 1 through Point 4. The operating frequency is kept equal to the resonant frequency at 99.3kHz, and the average input power is kept at 70W during the test. As a result, the voltage gains and power efficiencies measured at Point 1 through Point 4 are (2.59, 88.1%), (3.43, 80.8%), (3.09, 80.8%) and (4.10, 74.3%), respectively. In addition, the corresponding r_d and the FOM values of Point 1 through Point 4 are (71.4, 24.6), (80.0, 19.1), (65.8, 17.5) and (90.9, 16.7), respectively. The average errors between the measured and the predicted value are 4.5% for the voltage gain and 2.2% for the efficiency. These values are within feasible tolerance level for a draft design. The experimental results demonstrate that the voltage gain, and power efficiency of the resonant energy link can be analyzed through the FOM-r_d plane even with variations in the load resistance and coupling coefficient.

It is also noticeable that Point 5 and Point 6 in Fig. 11 are expected to show the gain bifurcation phenomenon since the operating points are located in the upper-left region of the FOM-r_d plane. The theoretical background of this graphical interpretation was explained in Section II. B and in Appendix B. Specifically, Point 5 is the operating point where the coupling coefficient is maintained at 0.041 (distance 30cm). However, the load resistance is further reduced to 10Ω, which causes the over-loaded condition. Likewise, Point 6 is the operating point where the load resistance is fixed to 60Ω. However, the coupling coefficient is further increased to 0.212 (distance 9cm), which results in the over-coupled condition. Frequency analyses results of points 5 and 6 are shown in Figs. 12(a) and 12(b), respectively. The measurement results demonstrate that the occurrence of bifurcation can be predicted using the FOM-r_d plane analysis.

IV. Conclusion

This paper presents a novel graphical method based on the FOM-r_d plane for the series-series configuration of an IPT system. The proposed method makes it possible to intuitively design the energy links in consideration of the voltage gain and the power efficiency In addition, it is possible analyze the system under coil misalignments and load changes with this method. By applying the design method, a 100W wireless power transfer system was constructed to verify its effectiveness by measurements. In conclusion, the proposed method is expected to be valuable for use in the design and analysis of IPT systems. In the future, research that extends the graphical method to other configurations such as S-P, P-S, or P-P will be conducted.

Appendix

A. Derivation of Performance Indices

By applying three basic assumptions in this paper to (1), (2) can be simplified into:

$$\begin{bmatrix} \mathbf{V_i}/R \\ 0 \end{bmatrix} = \begin{bmatrix} 1 & jkQ \\ jk\dfrac{Q}{1+r_d} & 1 \end{bmatrix} \begin{bmatrix} \mathbf{I}_1 \\ \mathbf{I}_2 \end{bmatrix}. \tag{A1}$$

Solving (A1), two branch currents can be obtained as:

$$\mathbf{I}_1 = \frac{\mathbf{V_i}}{R}\frac{1+r_d}{k^2Q^2+1+r_d}, \tag{A2}$$

$$\mathbf{I}_2 = -j\frac{\mathbf{V_i}}{R}\frac{kQ}{k^2Q^2+1+r_d}. \tag{A3}$$

Thus, the output power is derived as:

$$P_{out} = \frac{1}{2}R_L\left|\mathbf{I_2}\right|^2 = \frac{1}{2}\frac{\left|\mathbf{V_i}\right|^2}{R_L}\frac{k^2Q^2{r_d}^2}{[k^2Q^2+(1+r_d)]^2}, \tag{A4}$$

which can be reduced to the voltage gain formula as follows:

$$M_{V,AC} = \frac{\sqrt{2R_LP_{out}}}{\left|\mathbf{V_i}\right|} = \frac{FOM\cdot r_d}{FOM^2+(1+r_d)} \tag{A5}$$

Similarly, the power efficiency is given by:

$$\eta = \frac{P_{out}}{P_{in}} = \frac{R_L\left|\mathbf{I_2}\right|^2}{R\left(\left|\mathbf{I_1}\right|^2+\left|\mathbf{I_2}\right|^2\right)+R_L\left|\mathbf{I_2}\right|^2} = \frac{FOM^2\cdot r_d}{(1+r_d)^2+FOM^2(1+r_d)} \tag{A6}$$

B. Derivation of Bifurcation Criterion

Based on [16], bifurcation does not occur when the following condition is met:

$$k < \frac{R_2+R_L}{Z_{o2}}. \tag{B1}$$

By assuming that the resonant energy links in the text are symmetric, the above equation is equivalent to:

$$k < \frac{R+R_L}{Z_o} = \frac{R+R_L}{QR}, \tag{B2}$$

This is further manipulated into:

$$kQ = FOM < 1+\frac{R_L}{R} = 1+r_d. \tag{B3}$$

If r_d is much larger than unity, (B3) is reduced to (5).

Acknowledgment

This work was supported by the 2016 Research Fund of University of Ulsan, Republic of Korea.

References

[1] Chwei-Sen Wang, G. A. Covic and O. H. Stielau, "Power transfer capability and bifurcation phenomena of loosely coupled inductive power transfer systems," *IEEE Trans. Ind. Electron.*, Vol. 51, No. 1, pp. 148-157, Feb. 2004.

[2] J. Sallan, J. L. Villa, A. Llombart, and J. F. Sanz, "Optimal design of ICPT systems applied to electric vehicle battery charge," *IEEE Trans. Ind. Electron.*, Vol. 56, No. 6, pp. 2140-2149, Jun. 2009.

[3] S. Chopra and P. Bauer, "Analysis and design considerations for a contactless power transfer system," in *Proc. IEEE 33rd INTELEC*, pp. 1-6, 2011.

[4] S. Raju, R. Wu, M. Chan, and C. P. Yue, "Modeling of mutual coupling between planar inductors in wireless power applications," *IEEE Trans. Power Electron*., Vol. 29, No. 1, pp. 481-490, Jan. 2014.

[5] X. Tang, J. Zeng, K. P. Pun, S. Mai, C. Zhang, and Z. Wang, "Low-cost maximum efficiency tracking method for wireless power transfer systems," *IEEE Trans. Power Electron.*, Vol. 33, No. 6, pp. 5317-5329, Jun. 2018.

[6] D. H. Tran, V. B. Vu, and W. Choi, "Design of a high-efficiency wireless power transfer system with intermediate coils for the on-board chargers of electric vehicles," *IEEE Trans. Power Electron.*, Vol. 33, No. 1, pp. 175-187, Jan. 2018.

[7] Z. Huang, S. C. Wong, and C. K. Tse, "Control design for optimizing efficiency in inductive power transfer systems,"

IEEE Trans. Power Electron., Vol. 33, No. 5, pp. 4523-4534, May 2018.

[8] F. Liu, Y. Yang, D. Jiang, X. Ruan, and X. Chen, "Modeling and optimization of magnetically coupled resonant wireless power transfer system with varying spatial scales," *IEEE Trans. Power Electron.*, Vol. 32, No. 4, pp. 3240-3250, Apr. 2017.

[9] T. Komaru, M. Koizumi, K. Komurasaki, T. Shibata, and K, Kano, "Parametric evaluation of mid-range wireless power transmission," *2010 IEEE International Conference on Industrial Technology*, pp. 789-792, 2010.

[10] H. Sugiyama, "Optimal designs for wireless resonant energy link with symmetrical coil pair," *2011 IEEE MTT-S International Microwave Workshop Series on Innovative Wireless Power Transmission*: *Technologies, Systems, and Applications*, pp. 247-250, 2011.

[11] A. O. Anele, Y. Hamam, L. Chassagne, J. Linares, Y. Alayli, and K. Djouani, "Computation of the mutual inductance between air-cored coils of wireless power transformer," *J. Physics: Conference Series,* Vol. 633, No. 1, 2015.

[12] J. P. K. Sampath, A. Alphones, and D. M. Vilathgamuwa, "Figure of merit for the optimization of wireless power transfer system against misalignment tolerance," *IEEE Trans. Power Electron.*, Vol. 32, No. 6, pp. 4359-4369, Jun. 2017.

[13] W. Zhang, S. C. Wong, C. K. Tse, and Q. Chen, "Design for efficiency optimization and voltage controllability of series–series compensated inductive power transfer systems," *IEEE Trans. Power Electron*., Vol. 29, No. 1, pp. 191-200, Jan. 2014.

[14] C. H. Jeong, H. S. Choi, and S. J. Choi, "FOM-r_d plane: An effective design and analysis methodology for resonant energy link in inductive power transfer," *2017 IEEE Energy Conversion Congress and Exposition (ECCE),* pp. 4030-4034, 2017.

[15] F. W. Grover, *Inductance Calculations: Working Formulas and Tables*, Van Nostrand, New York, 1946

[16] P. E. K. Donaldson, "Frequency-hopping in r.f. energy-transfer links," *Electron. & Wireless World*, pp. 24-26, Aug. 1986.

Chae-Ho Jeong was born in Ulsan, Korea. He received his B.S. and M.S. degrees in Electrical Engineering from the University of Ulsan, Ulsan, Korea, in 2017 and 2019, respectively. He is an Assistant Research Engineer with G-Philos Company, Yongin, Korea. His current research interests include modeling and control of wireless power transfer systems.

Sung-Jin Choi received his B.S., M.S. and Ph.D. degrees in Electrical Engineering from Seoul National University, Seoul, Korea, in 1996, 1998 and 2006, respectively. From 2006 to 2008, he was a Research Engineer with Palabs Co., Ltd., Seoul, Korea. From 2008 to 2011, he was a Principal Research Engineer at Samsung Electronics Co., Ltd., Suwon, Korea, where he was responsible for developing LED drive circuits and wireless battery charging systems. In 2011, he joined the University of Ulsan, Ulsan, Korea, where he is presently working as an Associate Professor in the School of Electrical Engineering. From 2017 to 2018, he was a Visiting Scholar at San Diego State University, San Diego, CA, USA. His current research interests include power processing technology related to solar power generation, battery management and wireless power transfer.